

Growth kinetic study of Sputter Deposition: Ag on Si/SiO₂.

S. Banerjee and S. Kundu.

Surface Physics Division, Saha Institute of Nuclear Physics,
1/AF Bidhannagar, Calcutta 700064, India.

We have presented the kinetic study of the very initial growth stages of an ultra thin film (40Å - 150Å) of Ag sputter-deposited on Si(001) substrate containing native oxide using grazing incidence x-ray reflectivity (GIXR) technique and Atomic Force Microscopy (AFM). We observe that the film consists of mounds with the presence of voids. The thickness ' d_{xray} ' and the packing fraction ' η ' of the film as a function of time ' t ' follow a simple power law, $d_{xray} \sim t^m$ and $\eta \sim t^n$ with the exponent $m = 0.58$ and $n = 0.37$ respectively. We have quantitatively determined that the voids between the mounds decrease at the initial growth stages with the increase in mound size using GIXR measurement. The mound size increases mainly by the coalescence process on the substrate. We have observed that as a function of time the mound size $R(t)$ increases radially as $\sim t^z$. The radial growth exponent z crosses over from $z > 0.5$ to $z \sim 0.25$ indicating two growth regimes. The GIXR measurement reveals sublinear dependence of η on d and the AFM measurement shows a cross over of the radial growth exponent, both these indicates that the lateral growth of the mound is enhanced initially reducing the voids.

PACS numbers: 81.15.Cd, 68.55.Ac, 68.37.Ps, 61.10.Kw

e-mail: sangam@cmp.saha.ernet.in

The study on the growth of ultra thin metallic films are of great importance not only for understanding the growth kinetics at its fundamental level but also for its technological application in the fabrication of nano-devices. In the semiconductor industries, sputtering is commonly used for depositing ultra thin films for metallization. Here we report a study on the growth kinetics of the initial growth stages of Ag films using grazing incidence x-ray reflectivity (GIXR) technique and Atomic Force Microscope (AFM). GIXR technique has been successfully used in a non-destructive manner to obtain the structure and chemical profile of the film as a function of its depth [1–3]. Atomic force microscope (AFM) is used for obtaining topographic images of hard and soft surfaces with Angstrom resolution. Recently we have reported that when Ag is deposited using dc magnetron sputtering, the initial growth of the film is carpet-like and above a critical thickness ~ 40 Å the film structure changes to form mounds [4]. Below the critical thickness (~ 40 Å) one can easily modify the ultra thin film of Ag intentionally by the tip of AFM to fabricate periodic pattern of nanoscale order [4,5] and above the critical thickness of the film one observes the onset of mound formation and these mounds are significantly stable and cannot be modified by the AFM tip. The morphological shape of the mound could be determined by combining AFM and GIXR measurement [6]. In the present investigation we have studied the growth kinetics of ultra thin Ag film and the coarsening process of the mounds by following its evolution with respect to the deposition time using ex-situ AFM and GIXR measurement.

Formation of mounds in the initial growth stages of thin films of various materials have been observed earlier [7–14] and extensive theoretical work [15–17] have been carried out in particular for understanding the radial coarsening law $R(t) \sim t^z$ for the increase of the typical mound size R with respect to time ‘ t ’ which are observed in experiments [7–10,13] and simulations [18,19]. Most of the experimental work reported to our knowledge is based on film having thickness greater than the present study [7–14] and also grown using molecular beam epitaxy (MBE) [7–10]. Only a few studies on the kinetics of mound growth of sputter deposited Pt [12], Au [14], Ag [11] and TiN [13] films have been reported earlier. The kinetics of the growth of the mounds can be different in the case of films deposited using magnetron

sputtering than that grown using MBE. The present investigation will be of interest for comparing the growth of the sputter deposited film with that grown using MBE. In this letter we would like to address mainly the issue of time dependent coarsening of the mound using GIXR and AFM measurement. We have observed that mound size increases with time mainly by coalescence process and tried to look into the kinetic of its growth. We would also like to emphasise here that the film grown by sputtering techniques exhibits similar exponents only after certain initial stage of the film growth as predicted by certain theories [15–17] and by the films grown by MBE [7–10]. At the very initial stages of the film growth by sputtering technique we observe a higher value of growth exponent.

For the present work we have deposited thin films of silver (99.99 %, Target Material Inc.) on Si(001) substrate using a dc magnetron sputtering unit (Pfeiffer, PLS500). The sample preparations and deposition parameters are given in our earlier work, see reference [4,5]. Six different films were deposited as a function of time ($t = 20, 30, 40, 60, 120, 180$ secs.) for obtaining various thicknesses labeled as sample (a) to sample (f). The film thicknesses were measured using x-ray reflectivity technique [20]. For x-ray reflectivity measurement we have used $\theta - 2\theta$ diffractometer (Microcontrol Inc.). The Cu- $K_{\alpha 1}$ x-ray was obtained from 18KW rotating anode x-ray generator (Enraf Nonius Inc.). For obtaining the surface morphology of the film we have used atomic force microscope (Park Scientific Inc.). The scan was carried out using the AFM in contact mode and the z-calibration of the piezo was done using x-ray reflectivity measurement [21]. The measurements were carried out in air at room temperature.

We have used x-ray reflectivity technique to characterise the thickness and average electron density (AED) of the films. The AED of the film is related to mass and volume density of the film [1]. The x-ray reflectivity data has been presented by the authors recently [4,5], but the following analysis has not been presented earlier. The thickness ' d_{xray} ' and the packing fraction ' η ' obtained from the x-ray reflectivity data analysis are plotted as a function of deposition time ' t ' and are shown in fig.1(a) and 1(b) respectively. Both follow a simple power law relation $d_{xray} \sim t^m$ and $\eta \sim t^n$ with the exponent $m = 0.58$ and $n = 0.37$

respectively, obtained from the non-linear least square fitting (shown as solid line in fig. 1). The lower value of the exponent for the case of η implies that at the very initial growth stages the increase of packing fraction is more dominant than the increase of thickness as a function of time indicating that the deposited particle tries to spread laterally reducing the *voids* much faster than growing vertically for increasing the thickness of the film. A linear fit to the data plotted with its logarithmic values are also shown in the insets for better clarity. From the previous two power laws one can write a relation between η and d as $\eta \sim d^p$ where $p = n/m$. Using the values of m and n obtained from the fits, $p = 0.64$ and fig 1(c) shows this plot. The sublinear dependence of η vs d also indicates that the packing fraction grows faster initially than the thickness. Thus in the sputter deposition process of Ag on Si/SiO₂ the mound grows more rapidly in the lateral direction initially than vertically. The above growth mechanism indicates that the growth of the film by sputter deposition at its initial growth stages is very similar to Stranski-Krastanov type of growth [22].

AFM images for the six different samples and the typical line profiles for each of the images are shown in fig. 2 and fig. 3 respectively. The grain "mound" size can be estimated from the line profiles. We observe from the AFM image (fig.2a) and from the line profile (fig. 3a) that for sample (a) the mounds are monodispersed. As the time of deposition increases the mound size increases as marked by arrows in the line profile and labeled as "A" in the AFM images and in the line profiles. The number density of the mound decreases as the growth of the film continues, this indicates that the mound grows by coalescence process. Some "A" types mounds coalesce to form bigger mounds and are labeled as "B". As the deposition progresses further we observe in the case of sample (f) that there are now mainly three types of mound sizes and are marked as A, A1 and B in the AFM image. A1 is an intermediate-size mound, formed by the coalescence of mounds with fewer nearest neighbours. Many such intermediate size of mounds will develop from this instant and this makes us difficult to keep the track of the mounds size as a function of time and thus we have stopped the growth beyond this time. This indicates, that as the time progresses the size distribution changes from mono-dispersed to polydispersed. We are concentrating in

the present work only on the initial growth stages and hence we have selected mainly the two types of mounds A and B. We have plotted the mound size of type A and type B as a function of time in fig. 4. We observe that as a function of time the mound size $R(t)$ increases as $\sim t^z$, where the radial growth exponent z crosses over from a linear regime $z \sim 1$ to $z \sim 1/4$ for the mound type A and for the mound type B the exponent z crosses over from $z \sim 0.7$ to $z \sim 1/4$ at the same instant of time, indicating that there are two growth regimes during the coarsening process for the film grown using sputtering technique. The cross over of the exponent for both the cases occurs at the same time i.e., at time $t = 60$ secs. (This time depends on the growth conditions). The higher value of the exponent at small time 't' indicates that the mound growth in the radial direction is enhanced and beyond time $t = 60$ secs the radial growth is suppressed. The enhanced radial growth region and the suppressed radial growth region are shown in fig. 4. Thus, the analysis of the AFM results give similar interpretation as that obtained from the analysis of the x-ray reflectivity data. We can also infer from the above analysis that the growth of both the type of mounds (type A and type B) follows more or less a similar growth exponent (i.e., for $t < 60$ s the growth exponent $z > 0.5$ and for $t > 60$ s the value $z < 0.5$ for both the type of mounds).

We now look into the scaling aspects during the dynamic growth process. We have determined the rms roughness $w(t) = \langle [h(r, t) - \langle h \rangle]^2 \rangle^{1/2} \propto t^\beta$ for $r \gg \xi(t)$. The average $\langle \dots \rangle$ is the spatial average over the sample surface, h is the height on the surface separated by a lateral distance r and $\xi(t)$ is the lateral correlation length which is a measure of the average mound size. The $\xi(t) \sim t^z$, where $z = \beta/\alpha$, β being the growth exponent and α is the roughness exponent [23]. In the inset of fig. 4 we have plotted $w(t)$ vs t in a log-log scale and we again observe the power law dependence as $w(t) \sim t^\beta$ where $\beta \sim 0.75$ for $t < 60$ s and $\beta \sim 0.15$ for $t > 60$ s. This also clearly indicates that there are two different regimes of mound growth (Beyond $t = 60$ s we observe reduction of rms roughness). Recent theoretical work predicts that the characteristic length $\xi(t)$ scales as $\xi(t) \sim R(t) \sim t^z$ where $z \sim 1/4$ [15–17]. We see from fig. 4 that $R(t)$ follows the theoretical prediction for $t > 60$ s only. For the very initial growth stages which has not been studied carefully both experimentally and

theoretically, we observe that the radial (mound) growth exponent exhibits a higher power law. Thus, at the initial growth stages we observe a cross over of the radial growth exponent indicating that when the substrate surface is fully covered up by the mounds suppressing the substrate effects the lateral growth of the mound is also suppressed. We would like to make a remark here that we have not used the roughnesses obtained from the specular x-ray reflectivity for the above plot of $w(t)$ vs t (inset of fig. 4). Recently one of the author has pointed out that the parameter σ [24] which is the FWHM of the gaussian distribution of the derivative of the electron density ' $d\rho(z)/du$ ' where $\rho(u)$ is the electron density as a function of depth u of the film which most often is termed as roughness may not be the true roughness w as defined above [25].

In conclusion, we have presented a comprehensive picture of film growth by sputtering deposition. We have followed the growth kinetics of the initial growth stages of Ag film grown by sputter deposition using GIXR and AFM measurements. We have proposed coalescence process as the growth mechanism for the increase of mound size as a function of time during the growth of the film. We have observed cross over of the radial growth exponent of the mounds indicating that there exist two distinct growth regimes. As a function of time during the growth of the film, initially the mound in the film exhibits enhanced lateral growth showing higher value of radial growth exponent and as the time progresses the lateral growth is suppressed. The two regimes have different kinetics of growth. The mound growth exponent $z \sim 1/4$ agrees with the theoretical and the simulation prediction for the later stages of growth when the substrate effect is suppressed.

REFERENCES

- [1] S.Banerjee, M.K.Sanyal, A.Datta, S.Kanakaraju and S.Mohan, Phys. Rev. B **54** 16377 (1996), S.Banerjee, A.Datta and M.K.Sanyal, Vacuum **60**(4) 371 (2001)
- [2] S.Banerjee, G.Raghavan and M.K.Sanyal, J. App. Phys. **85** 7135 (1999)
- [3] J. K. Basu, M. K. Sanyal, M. Mukherjee and S. Banerjee, Phys. Rev. B **62**, 11109 (2000)
- [4] S.Banerjee, S. Mukherjee and S. Kundu, J. Phys. D: Appl. Phys. **34**, L87 (2001)
- [5] S. Banerjee, S.Mukherjee and S. Kundu (submitted)
- [6] S. Kundu, S. Hazra, S. Banerjee, M. K. Sanyal, S. K. Mandal, S. Chaudhuri and A. K. Pal, J. Phys. D: Appl. Phys. **31**, L73 (1998)
- [7] M. G. Gyure, J. J. Zinck, C. Ratsch and D. D. Vvedensky, Phys. Rev. Lett, **81**, 4931 (1998)
- [8] J.A.Stroschio, D. T. Pierce, M. D. Stiles A. Zangwill and L. M. Sander, Phys. Rev.Lett. **75**, 4246 (1995)
- [9] G. Lengel, R. J. Phaneuf, E. D. Williams, S. Das Sarma, W. Beard and F. G. Johnson, Phys. Rev. B **60**, R8469 (1999)
- [10] G. Apostolopoulos, J. Herfort, L. Daweritz K. H. Ploog and M. Luysberg, Phys. Rev. Lett. **84**, 3358 (2000)
- [11] J. H. Je , T. S. Kang and D. Y. Noh, J. Appl. Phys. **81**, 6716 (1997)
- [12] J. H. Jeffries, J.-K. Zuo and M. M. Craig, Phys. Rev. Lett. **76**, 4931 (1996)
- [13] B. W. Karr, I. Petrov, D. G. Cahill and J. E. Greene, Appl. Phys. Lett. **70**, 1703 (1997)
- [14] H. You, R. P. Chiarello, H. K. Kim and K. G. Vandervoort, Phys. Rev. Lett. **70**, 2900 (1993)
- [15] M. Siegert, Phys. Rev. Lett. **81**, 5481 (1998), M. Siegert, M. Plischke and R. K. P. Zia,

- Phys. Rev. Lett. **78**, 3705 (1997), M. Siegert and M. Plischke, Phys. Rev. Lett. **73**, 1517 (1994).
- [16] M. Rost and J. Krug, Phys. Rev. E **55**, 3952 (1997)
- [17] J. G. Amar, Phys. Rev. B **60**, R11317 (1999)
- [18] P. Smilauer, M. Rost and J. Krug, Phys. Rev. E **59**, R6263 (1999)
- [19] M. D. Johnson, C. Orme, A. W. Hunt, D. Graff, J. Sudijono, L. M. Sander and B. G. Orr, Phys. Rev. Lett. **72**, 116 (1994)
- [20] M. Born and E. Wolf, Principles of Optics (6th edition, Oxford: Pergamon, 1980)
- [21] S. Pal and S. Banerjee, Rev. Sci. Instrum. **71**, 589 (2000)
- [22] Th. Schmidt and E. Bauer, Phys. Rev. B **62**, 15815 (2000)
- [23] A-L. Barabasi and H. E. Stanley, *Fractal Concepts in Surface Growth* (Cambridge University Press, Cambridge, England, 1995)
- [24] L. Nevot and P. Croce, Rev. Phys. Appl. **15**, 761 (1980)
- [25] S. Banerjee, A. Gibaud, D. Chateigner, S. Ferrari and M. Fanciulli, J. Appl. Phys. (in press, 2001)

Figure Captions:

FIG. 1. Time evolution of (a) thickness ‘ d ’, and (b) packing fraction ‘ η ’ for the sputter deposited Ag films. The solid lines shows that both follows a simple power law, $d_{xray} \sim t^m$ and $\eta \sim t^n$ with the exponent $m = 0.58$ and $n = 0.37$ respectively. The packing fraction η is related to d as $\eta \sim d^p$ where $p = n/m = 0.64$, the solid line shows the plot. In insets we have plotted the logarithmic values and we show the linear fit for better clarity.

FIG. 2. AFM images for sample (a) to sample (f). As the time of deposition increases the mound size increases by coalescence process labeled as “A”. Some A type mounds coalesces to form mounds of type B and A1 are the mound at later stages. The solid lines in the images are the marker for the line profiles and the respective arrows are shown in FIG. 3.

FIG. 3. Typical line profiles for sample (a) to sample (f) marked as solid lines in the AFM images of FIG. 2. The arrows indicated by label “A” are for mounds of type A and label “B” are for mounds of type B.

FIG. 4. The time evolution the radial mound size $R(t)$ increases radially as $\sim t^z$. The radial growth exponent z crosses over from a linear regime $z \sim 1$ to $z \sim 1/4$ for mound A and from $z \sim 0.7$ to $z \sim 1/4$ for mound B at the same instant of time $t = 60s$ indicating two growth regimes. The two growth regimes are marked by a vertical dash line seperating the enhanced lateral growth regime from the suppressed lateral growth regime. The inset shows the rms roughness $w(t) \sim t^\beta$ where the growth exponent $\beta \sim 0.75$ for $t < 60s$ and $\beta \sim 0.15$ for $t > 60s$ showing different values in both the regimes.

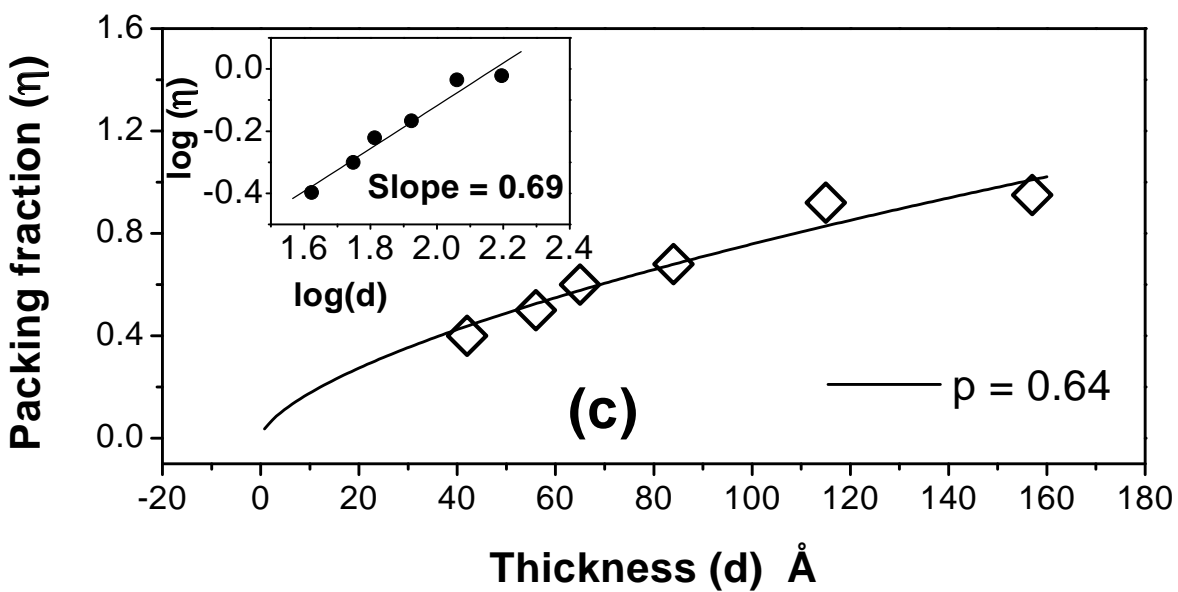
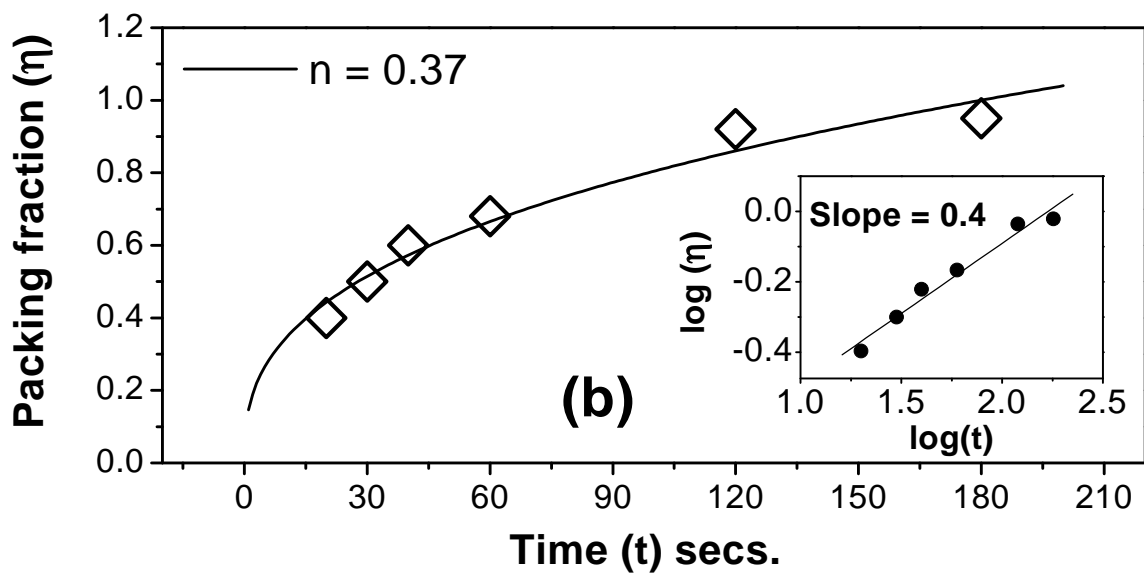
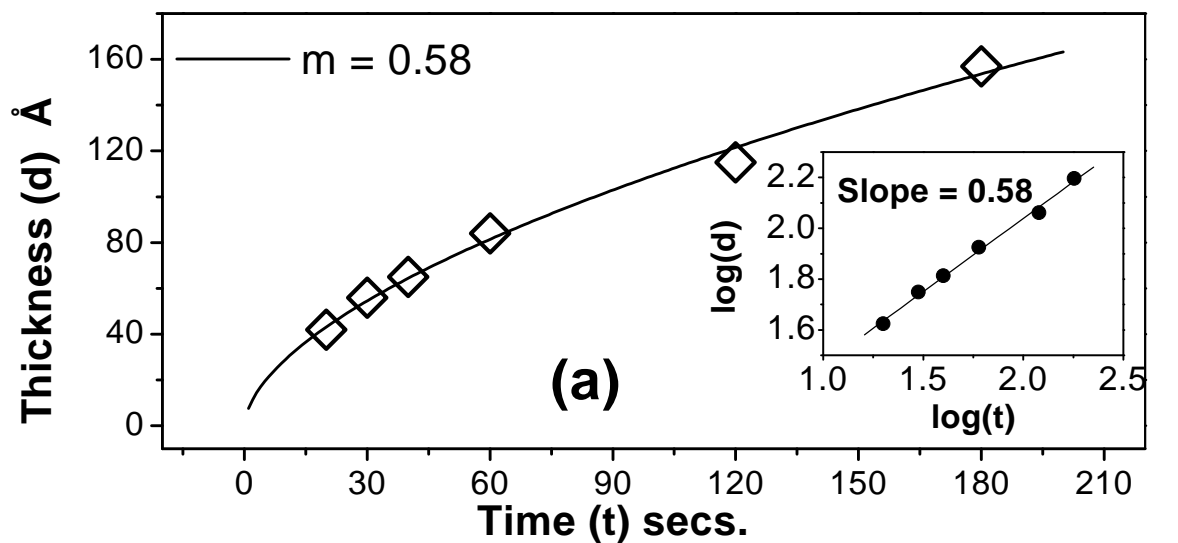


Fig. 1 (S. Banerjee and S. Kundu)

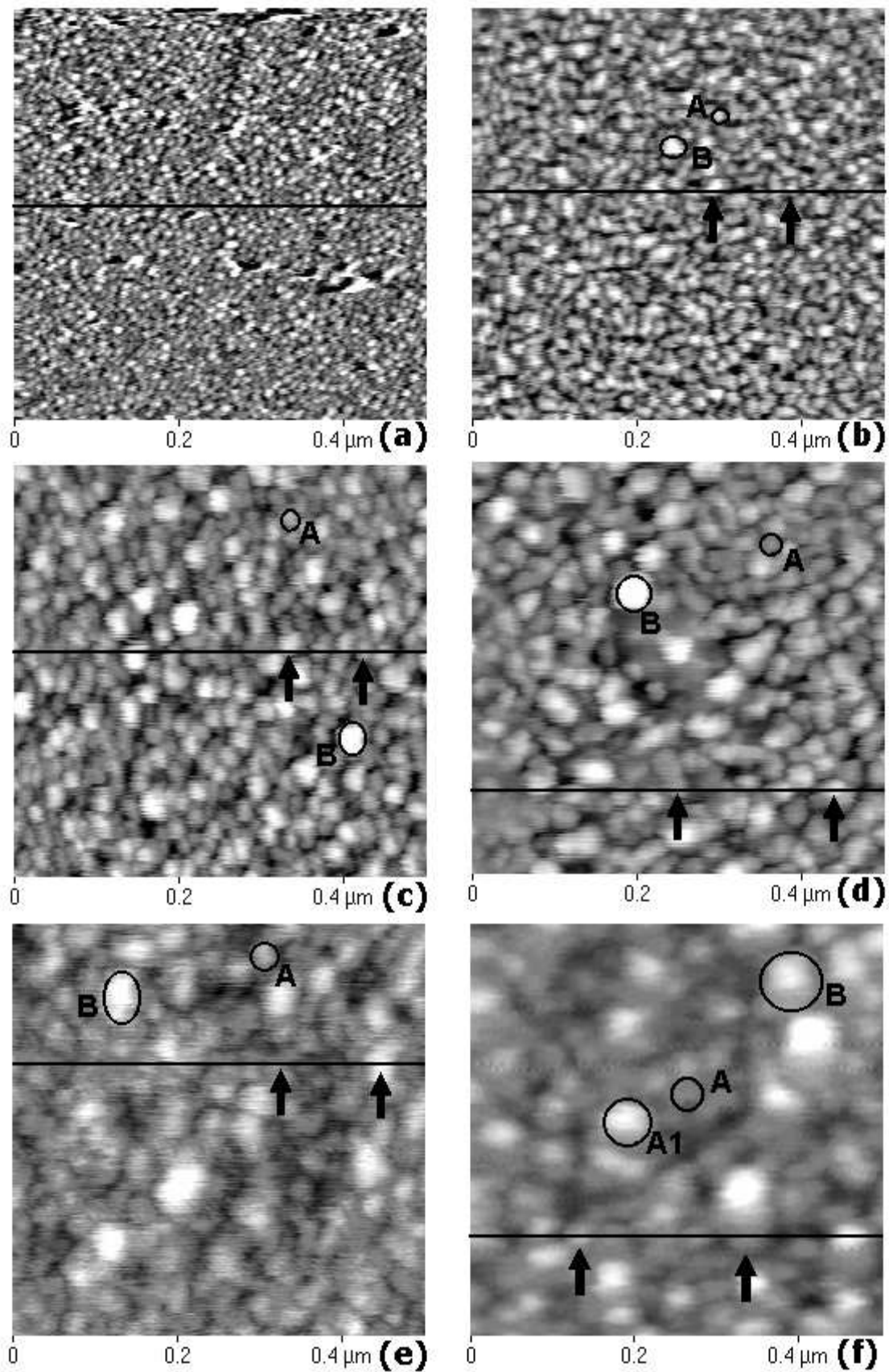


Fig. 2 (S. Banerjee and S. Kundu)

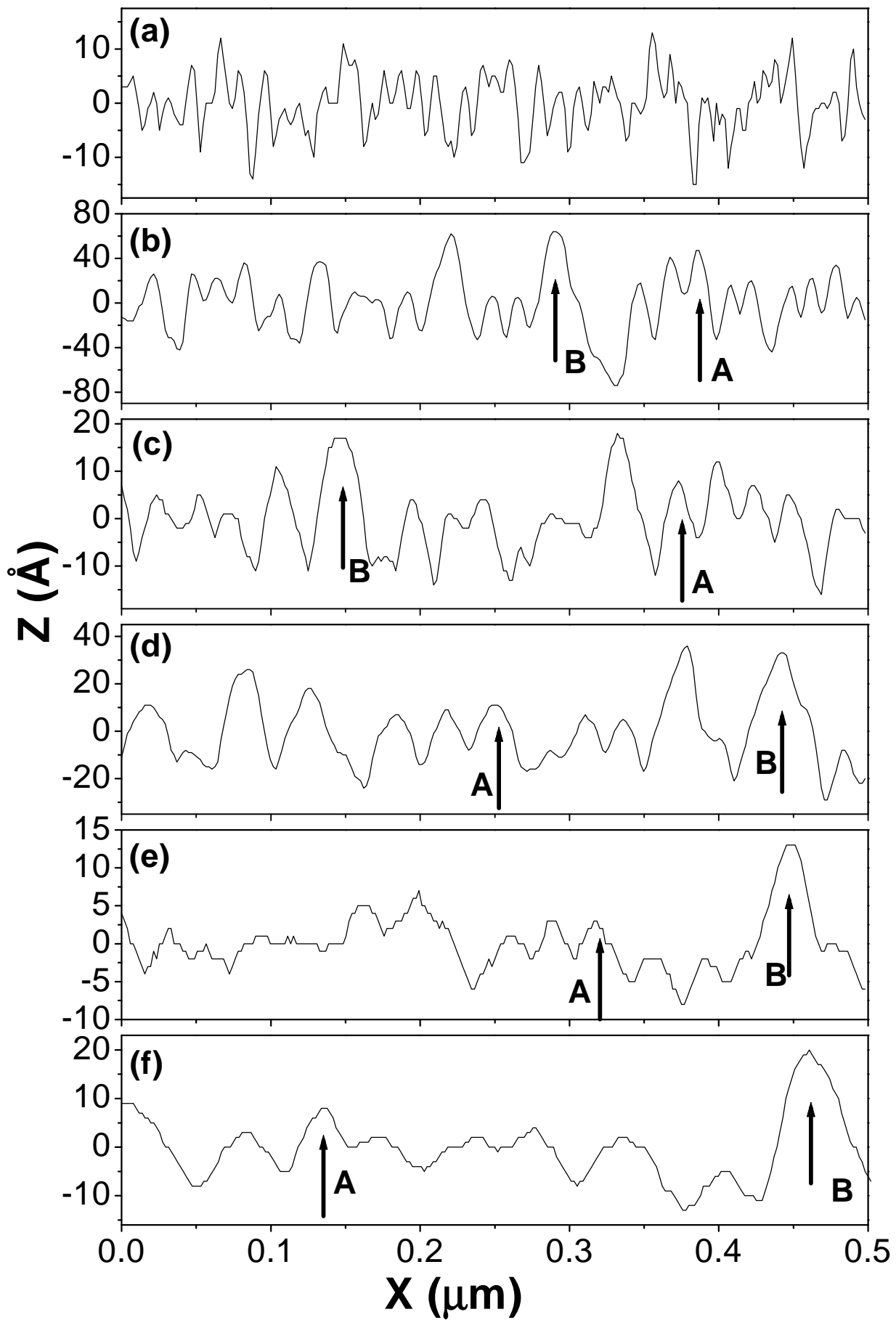


Fig. 3 (S. Banerjee and S. Kundu)

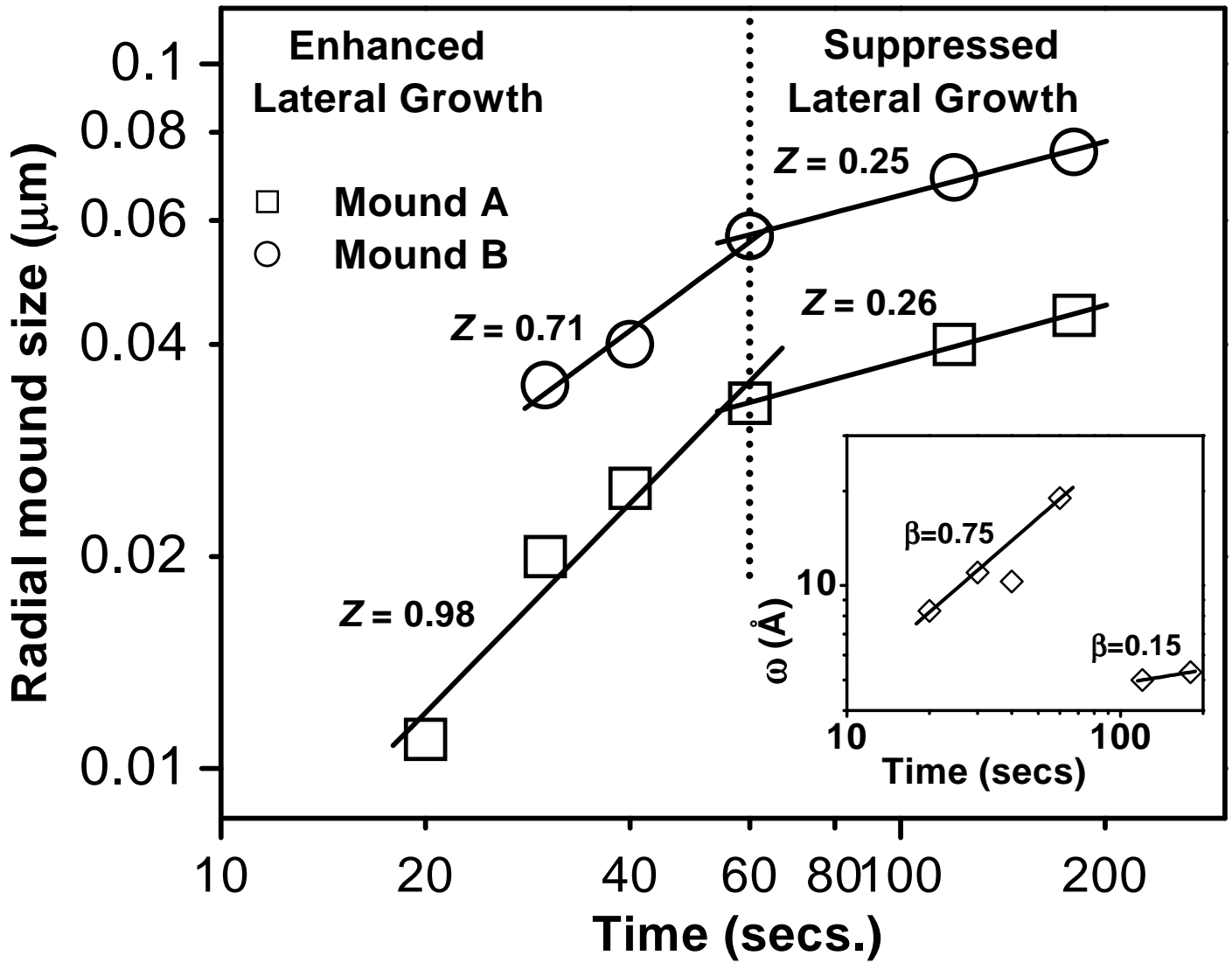


Fig. 4 (S. Banerjee and S. Kundu)